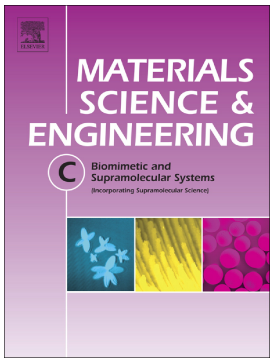

Immunosensors containing solution blow spun fibers of poly(lactic acid) to detect p53 biomarker

Andrey Coatrini Soares, Juliana Coatrini Soares, Rafaella Takehara Paschoalin, Valquiria Cruz Rodrigues, Matias Eliseo Melendez, Rui M. Reis, André Lopes Carvalho, Luiz Henrique Capparelli Mattoso, Osvaldo N. Oliveira

PII: S0928-4931(19)34046-9

DOI: https://doi.org/10.1016/j.msec.2020.111120

Reference: MSC 111120

To appear in: *Materials Science & Engineering C*

Received date: 9 November 2019

Revised date: 22 April 2020

Accepted date: 24 May 2020

Please cite this article as: A.C. Soares, J.C. Soares, R.T. Paschoalin, et al., Immunosensors containing solution blow spun fibers of poly(lactic acid) to detect p53 biomarker, *Materials Science & Engineering C* (2020), https://doi.org/10.1016/j.msec.2020.111120

Immunosensors Containing Solution Blow Spun Fibers of Poly(Lactic Acid) to Detect p53 Biomarker

Andrey Coatrini Soares[a,b], Juliana Coatrini Soares[a], Rafaella Takehara Paschoalin[b], Valquiria Cruz Rodrigues[b], Matias Eliseo Melendez[c], Rui M. Reis[c,d,e], André Lopes Carvalho[c], Luiz Henrique Capparelli Mattoso[a,f], Osvaldo N. Oliveira Jr[b*]

[a] Nanotechnology National Laboratory for Agribusiness (LNNA), Embrapa Instrumentation, 13560-970 São Carlos, SP, Brazil

[b] São Carlos Institute of Physics, University of São Paulo, 13566-590 São Carlos, Brazil

[c] Molecular Oncology Research Center, Barretos Cancer Hospital, 14784-400 Barretos, Brazil

[d] Life and Health Sciences Research Institute (ICVS), School of Medicine, University of Minho, 4710-057 Braga, Portugal.

[e] ICVS/3B's - PT Government Associate Laboratory, 4805-017 Braga, Portugal.

[f] Materials Engineering Department, Federal University of São Carlos, 13565-905 São Carlos, Brazil

*Corresponding Author: Osvaldo N. Oliveira Jr
E-mail: chu@ifsc.usp.br

Abstract

This paper reports on biosensors made with a matrix of polylactic acid (PLA) fibers, which are suitable for immobilization of the anti-p53 active layer for detection of p53 biomarker. The PLA fibers were produced with solution blow spinning, a method that is advantageous for its simplicity and possibility to tune the fiber properties. For the biosensors, the optimized time to deposit the fibers was 60 s, with which detection of p53 could be achieved with the limit of detection of 11 pg/mL using electrical impedance spectroscopy. This sensitivity is also sufficient to detect the p53 biomarker in patient samples, which was confirmed by distinguishing samples from cell lines with distinct p53 concentrations in a plot where the impedance spectra were visualized with the interactive document mapping (IDMAP) technique. The high sensitivity and selectivity of the biosensors may be attributed to the

specific interaction between the active layer and p53 modeled with a Langmuir-Freundlich and Freundlich isotherms and inferred from the analysis of the vibrational bands at 1550, 1650 and 1757 cm^{-1} using polarization-modulated infrared reflection absorption spectroscopy (PM-IRRAS). The successful immobilization of the active layer is evidence that the approach based on solution blown spun fibers may be replicated to other types of biosensors.

Keywords: PLA Fibers, Solution Blow Spinning, Immunosensor, Cancer, p53.

1) Introduction

The concept of nanoarchitectonics[1–3] has become increasingly popular for it encompasses many ways of controlling molecular architectures in materials where synergy is sought to enhance properties for specific applications[4]. Biosensing, for instance, is now mostly based on layered architectures with tuning of composition in both the active layer and its underlying matrix[4,5]. Though only a few techniques are employed to build the nanostructured films comprising the biosensors, *e.g.* the Langmuir-Blodgett (LB)[6], layer-by-layer (LbL)[7] and self-assembled monolayer (SAM)[8,9] methods, the variety of materials and possible architectures is immense[10]. The key features for choosing the molecular architectures are the ability to preserve activity of the biomolecules in the active layer and increase the sensing signal, which may be optical, electrical and mechanical, depending on the principle of detection.

One challenging application for biosensors is the early diagnosis of diseases such as cancers, normally done by detecting biomarkers in body fluids and tissues [11,12]. The rationale for using these biosensors is to replace the expensive, time-consuming methods based on molecular techniques such as polymerase chain reaction (PCR), especially for screening the population considered at risk. Many examples exist of immunosensors used to detect biomarkers, whose overexpression denotes possible development of cancer[13–16]. While the

composition of the active layer is defined by the intended antigen-antibody interaction, the choice of the matrix onto which the active layer is to be adsorbed can vary widely. There is no general rule as to which material makes the most suitable matrix, but evidence has been gathered that some renewable materials and nanomaterials are excellent in biosensing. These include chitosan[4,7], chondroitin sulfate[7], carbon nanotubes[13], graphene[17] and others. In many cases, in addition to preserving the activity of the biomolecules the matrix helps enhance the signal, as with the use of metallic nanoparticles in electrochemical sensors[18,19].

Among the many matrices used in biosensors, those obtained with electrospun nanofibers[20] have provided high performance. These fibers are advantageous because they form three-dimensional platforms that offer an electroactive biocompatible surface which assist in the active layer immobilization with suitable conformation and biological activity[21]. In fact, the fabrication can be even simpler if the fibers are deposited using solution blow spinning (SBS)[22–24]. This technique is a low-cost method to produce polymeric fibers, similar to electrospinning but not requiring sophisticated equipment, providing continuous fiber production with large surface area and high porosity[24]. Surprisingly, we were unable to find fibers matrices constructed with SB-Spinning technique for immunosensors.

In this paper, we report on immunosensors made with SB-Spinning matrices of polylactic acid (PLA) fibers with active layers of anti-p53 antibodies. The choice of p53 as the analyte was motivated by the availability of biosensing results in the literature to compare with the present work, and by the paramount role of p53 in tumorigenesis[25]. Indeed, p53 is a tumor suppressor gene located on the chromosome 17.2, whose inactivation results in mutations that cause various types of cancers, including breast, lung, skin and lymphomas[26]. Herein, detection of p53 is carried out using electrical impedance spectroscopy in commercial protein samples and cell line lysates. In order to optimize film fabrication conditions and establish a generic platform for the manufacture of other cancer biosensors, multidimensional

projection techniques along with specific surface analysis techniques were used to achieve high sensitivity and selectivity.

2) Experimental Section

2.1. Functionalization of Gold Interdigitated Electrodes with PLA Fibers

Gold interdigitated electrodes with 50 pairs of 10 μm wide electrodes, 10 μm apart from each other[5], were functionalized with poly(latic acid) (PLA) fibers (Mw = 76,000 g/mol, Sigma Aldrich). The fibers were deposited with the solution blow spinning method[22,24], in a setup comprising a syringe pump (New Era Syringe Pump) that injects the polymer into a system with internal and external nozzles. The feed rate of 7 mL/h is obtained by connecting these nozzles to an air compressor with 100-200 kPa pressure, which assists in drying and forming the fibers, depositing them on the electrodes attached to a cylindrical collector positioned horizontally (18 cm) from the nozzles. The collector rotates at 180 rpm, and in this work the deposition times used were 15, 30, 60 and 90s. The carboxylic acid groups of the deposited PLA fibers were activated by incubation in a solution 0.1 M of 1-ethyl-3- (3-dimethylaminopropyl) carbodiimide (M_W=155.24 g/mol) (EDC)/0.1 M N-hydroxysuccinimide (NHS) (M_W = 115.09 g / mol) for 30 min[8], and then coated with an active layer of anti-p53 antibodies adsorbed during 40 min. The final procedure to prepare the biosensor is the immersion into a 1% bovine serum albumin (BSA) solution for 30 min to block non-specific sites[4,5]. Figure 1 shows a schematic drawing of interdigitated electrodes coated with PLA fibers functionalized with antibodies to detect the p53 protein.

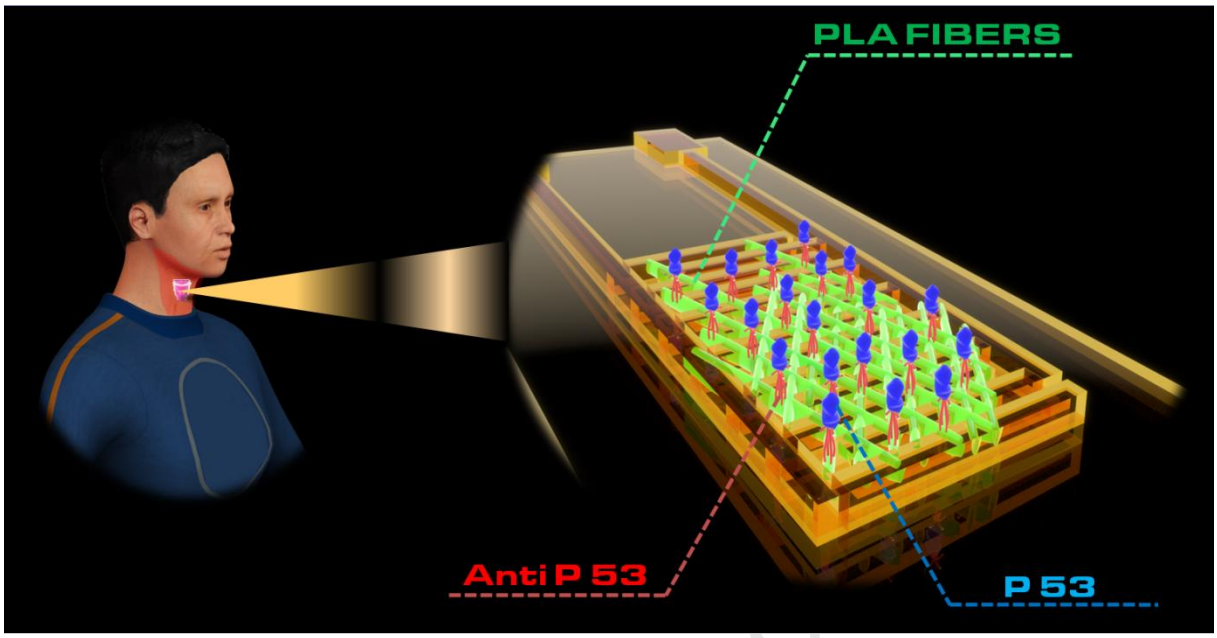

Figure 1: Preparation of interdigitated electrodes with PLA fibers functionalized with antibodies to detect the p53 protein

2.2. p53 Detection.

Measurements of electrical impedance spectroscopy were carried out using a Solartron model SI 1260 A, in the frequency range from 1 to 10^6Hz. The biosensors were exposed for 10 min in a p53 biomarker aqueous solution at various concentrations (0.05, 0.1, 0.6, 1.1, 1.6 and 3 ng/mL). This adsorption process was followed by washing the biosensor with PBS to remove poorly adsorbed molecules. The same procedure was used to evaluate the biosensor efficiency in detecting cell lysates from MCF7 breast cancer cell line (p53 expressing) with different concentrations (0.01, 0.1, 1, 10, 100, 500 and 1000 Ucell/mL), in addition to p53-null cells (Saos-2 osteosarcoma cell line) as negative controls. The capacitance spectra were used to construct calibration curves and calculate analytical parameters of the biosensors, such as the limit of detection, and to obtain visualization maps for distinguishing the different types of samples.

2.3. Data Analysis with Information Visualization Techniques

The capacitance spectra were analyzed using the software Projection Explorer Sensors (PEx-Sensors)[27], which generates interactive document maps (IDMAP)[27,28] and permits analysis using the parallel coordinate (PC) technique[29]. In IDMAP the Euclidean distance is calculated between the signal of samples $X=\{x_1, x_2, \ldots, x_n\}$ in the original space, as dissimilarity functions between two any samples. These data are projected into a lower space dimension, where $Y=\{y_1, y_2, ..., y_n)$ is the position of the visual elements and $d(y_i, y_j)$ is the function of the Euclidean distance between two elements of Y. These projections are injective functions f: X→Y that minimize the term $\left|\delta(x_i, x_j) - d(f(x_i) - f(x_j))\right| \forall x_i, x_j \in X$, and is given by eq. 1.

$$S_{IDMAP} = \frac{\delta(x_i, x_j) - \delta_{\min}}{\delta_{\max} - \delta_{\min}} - d(y_i, y_j) \quad (1)$$

where $\delta_{\max}$ and $\delta_{\min}$ are the maximum and minimum Euclidean between the data points

3. Results and Discussion

3.1. Characterization of PLA fibers

Polymer fibers made with SB-Spinning are advantageous to form a biosensor matrix because of the versatility in choosing deposition parameters, such as the time, which may permit tuning surface properties and facilitate adsorption of analytes. Herein, two characterization techniques were used to optimize the manufacturing conditions of PLA fibers. The scanning electron microscopy (SEM) images in Figures S1-A, S1-B and S1-C (Supporting Information) illustrate the increase in fiber concentration per unit area with deposition time, which produces a homogeneous film under optimized conditions on the surface of Au electrodes. These fibers have diameters of 274-688 nm in films produced within

15s, but become more uniform with deposition time. For the films obtained within 60 s, PLA fibers had diameters of 247-297 nm. As will be shown later on, the biosensing performance is related to the uniformity of the fibers which contributes to enhancing the analytical parameters with the increased availability of sites for adsorption of anti-p53 antibodies.

The adsorption of PLA fibers on interdigitated electrodes and the study of adsorption time are corroborated by Polarization-Modulation Infrared Reflection-Absorption Spectroscopy (PM-IRRAS), which confirms the intended functionalization of the electrodes. Figure 2A shows the characteristic bands of poly(lactic acid) (PLA) at 1215 cm^{-1} (–O-C-O stretching), 1269 cm^{-1} (–C=O deformation), 1358 cm^{-1} (symmetrical and asymmetric deformation of C-H) and 1757 cm^{-1} (-C=O carboxylic acid stretching)[30]. The intensity of these bands increases with deposition time, especially for the 1757 cm^{-1} band whose increase is depicted in Figure 2B. The increased amount of adsorbed material with the time of deposition may be important for the sensor characteristics, such as selectivity and sensitivity.

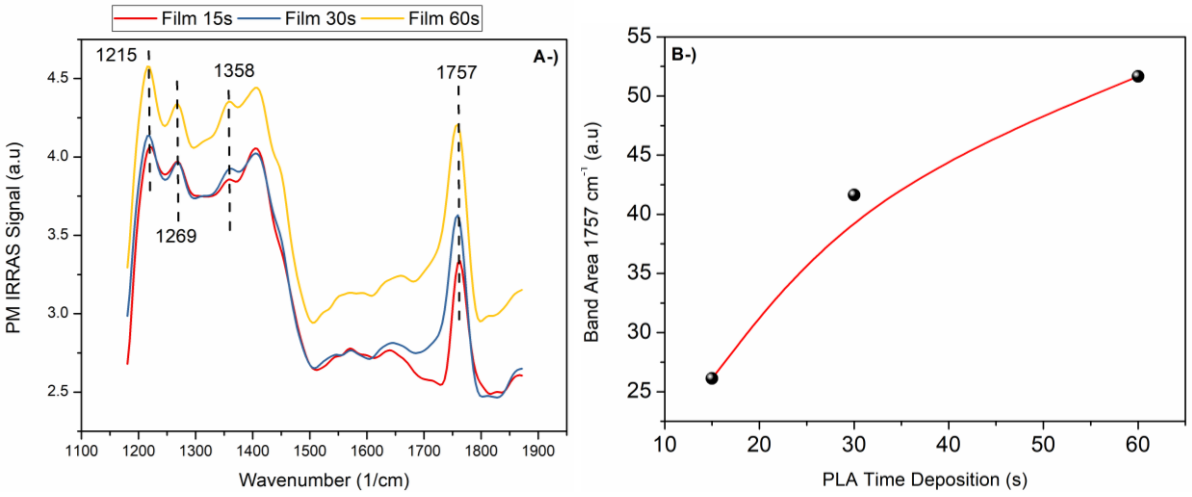

Figure 2: (a) PM-IRRAS spectra of PLA fibers deposited during 15, 30 and 60s; (b) Changes of the band area of C=O with increasing deposition time.

3.2. p53 Biomarker Detection in Commercial Samples

Electrical impedance spectroscopy was applied to detect p53 biomarker using the sensing units made with a matrix of PLA fibers described in Section 2.1. Figures 3a, 3b, 3c and 3d show the capacitance spectra for sensing units whose matrices were built with 15, 30,

60 and 90s, respectively. Changes in the capacitance spectra are best observed at frequencies below 10,000 Hz, where the electrical response is dominated by effects on the electrical double layer and changes in nanostructured films, induced by interaction mechanisms between antibodies and antigens[31,32]. The inserts in Figure 3 show the calibration curves from the capacitance values at 100, 215 and 1000 Hz for the sensors from PLA nanofibers deposited during 15, 30, 60 and 90s. These frequencies were chosen based on an analysis of biosensing performance employing the parallel coordinate technique to visualize the capacitance spectra, as discussed later on. The limits of detection (LoD) were calculated using IUPAC recommendation[7]. The number of available active sites tends to zero with the p53 concentration, because the AB-AG interaction was irreversible[4], thus yielding maximum detectable concentrations of *ca.* 1.6 ng/mL for sensors A, B and C, and 0.6 ng/mL for sensor D. The biosensors had LoD between 11 and 72.3 pg/mL, depending on the frequency and deposition time for the PLA fibers. LOD for the optimized biosensor built with a PLA matrix deposited during 60s is competitive with others in the literature[9], being sufficient to detect p53 in blood samples, since reference values are 30 pg/mL for lymphoma, 50 pg/mL for Hodgkin's lymphoma/bladder cancer/colon cancer/lung cancer and 200 pg/mL for ovarian cancer[9]. These sensors built with solution blow spun fibers of poly(Lactic Acid) have a much wider working range than the sensors built with electrically spun fibers[20].For PA6/PAH/MWCNT and PA6/PAH/AuNP sensors, the saturation of active sites occurs at a concentration up to 1.6x the reference value for detection of pancreatic cancer[20]. In contrast, with SB-Spinning sensors saturation occurs at a concentration up to 53x the reference values for detecting p53.

Optimized performance was observed for PLA fiber deposition of 60s because a more effective antibody anchoring occurred with increasing deposition time, as confirmed with PM-IRRAS data to be presented in Section 3.1. It should be noted, however, that above 60s

fiber deposition is not homogenous and the films make the surface nonconductive, thus hampering sensing performance. This should be expected from the literature since there is an optimized film thickness for biosensing performance, which is due to the competition between having more active materials to enhance biosensing and the reduced charge transport as the thickness increases[33]. The results are summarized in Table 1.

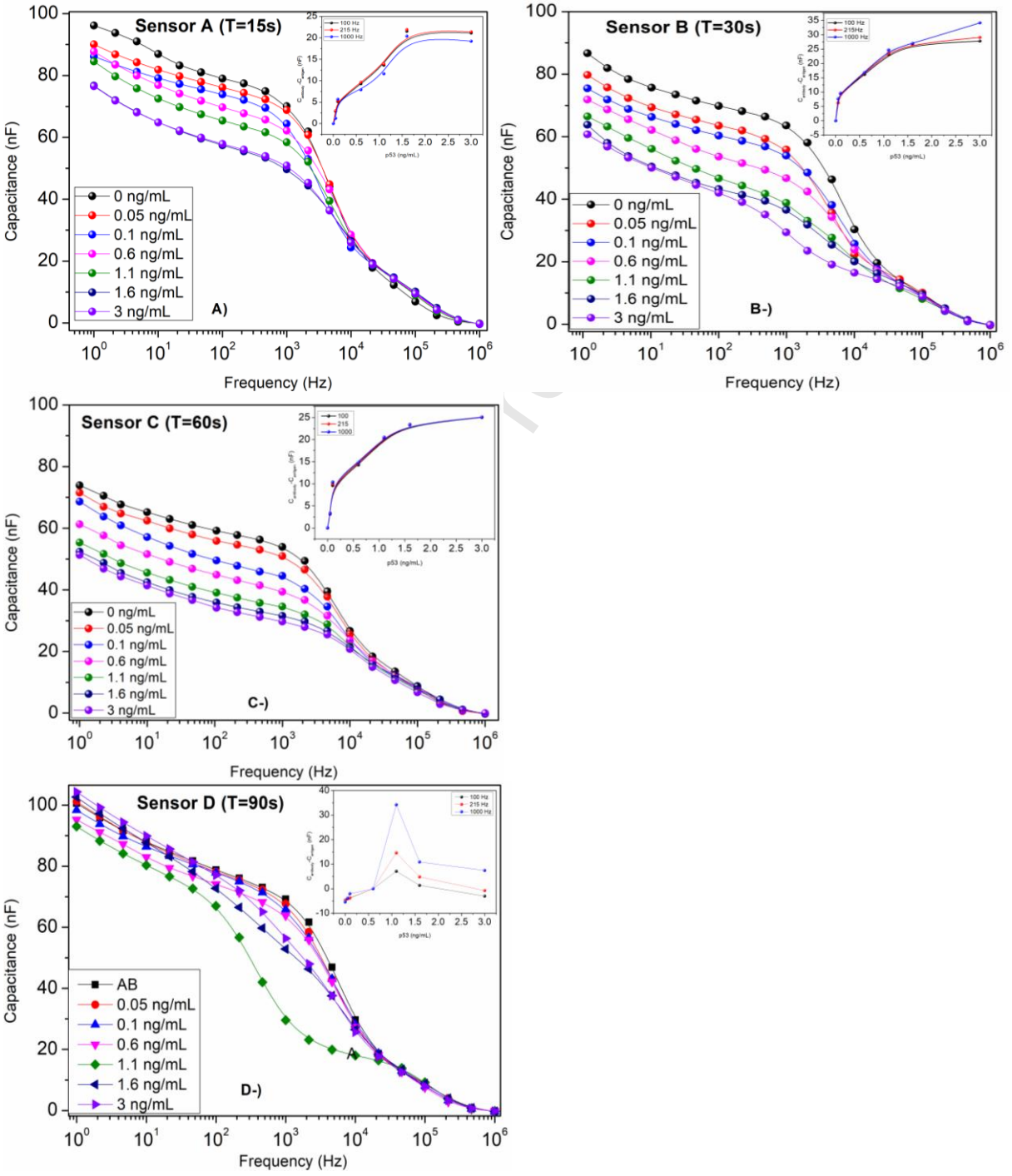

Figure 3: Capacitance spectra of biosensors constructed from PLA fibers, deposited during (A) 15s (biosensor A), (B) 30s (biosensor B), (C) 60s (biosensor C) and (D) 90s (biosensor D), immersed in PBS solution with different concentrations of p53 biomarker.

Table 1: Limits of detection (LoD) and working range for biosensors made with PLA fibers for 15, 30, 60 and 90s. Results are presented for capacitance measurements at 3 frequencies selected as the most suitable for distinction of the samples, according to the analysis using parallel coordinates and the silhouette coefficients.

Biosensor Label	Time of Deposition for the PLA Matrix	Angular Frequency (Hz)	LoD (pg/mL)	Range (ng/mL)
A	**15s**	100	72.3	0-1.6
		215	71.1	
		1000	59.1	
B	**30s**	100	28.6	0-1.6
		215	28.8	0-1.6
		1000	44.3	>3
C	**60s**	100	18.1	0-1.6
		215	14.2	
		1000	11.0	
D	**90s**	100	---	0-0.6
		215	---	
		1000	---	

The optimization of biosensor performance is critical to high-performance devices. We utilized two information visualization techniques to compare the performance of the biosensors. The first technique, referred to as Interactive Document Maps (IDMAP), converts the capacitance spectra into 2-D visualization maps, preserving the similarity of the original multidimensional space on a 2D space. The second technique permits one to evaluate the distinction ability based on capacitance values. A visual analysis of the map in Figure 4 shows that biosensor C has higher selectivity and sensitivity, with clear distinction among different

concentrations of p53 (orange region). For the other biosensors, distinction is not as clear, particularly for Biosensor D built with a PLA matrix deposited during 90s, where the data points are not positioned according to increasing p53 concentration.

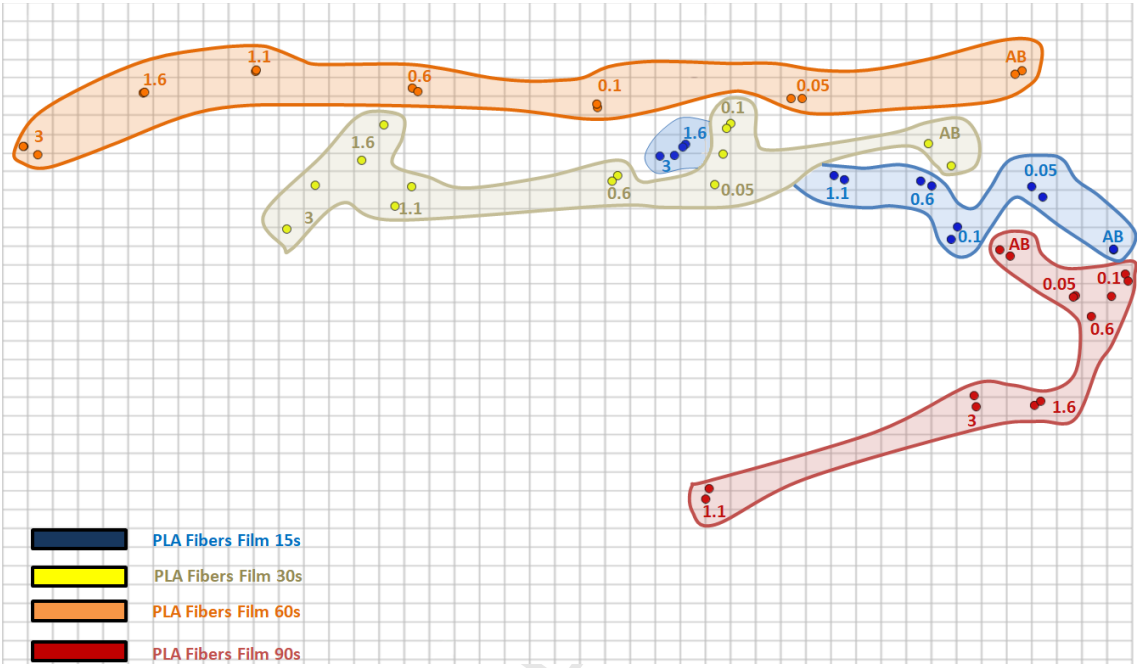

Figure 4: IDMAP plot with data from the commercial protein samples p53 for the biosensors A (blue), B (yellow), C (orange) and D (red). Each point represents a capacitance spectrum for each p53 concentration. The axes are not labeled because IDMAP calculates the relative Euclidean distance between the data points.

This selectivity can be quantified by the silhouette coefficient (S)[29], calculated using equation 2, where P is the number of samples, a_i is the average distance calculated between the i^{th} capacitance x frequency projection and the remaining capacitance x frequency curves projections and b_i is the minimum distance of the i^{th} projection and projections of other clusters with different concentrations[5].

$$S = \frac{1}{P}\sum_{i=1}^{n}\frac{(b_i - a_i)}{\max(b_i, a_i)} \qquad (2)$$

The value of the silhouette coefficient varies between -1 and 1 and is calculated individually at each frequency of the capacitance spectra projected on the parallel coordinate

graphs of Figure 5. These values are represented by blue, red and white boxes indicating, respectively, high coefficient (i.e, the capacitance at that frequency is useful for distinguishing the samples, with S ~ 1), low silhouette coefficient (S ~ -1, with data hindering distinction) and S ~ 0 (i.e. using the data is indifferent for distinction). For PLA fiber films, the average silhouette coefficients for sensors A, B, C and D were 0.725, 0.779, 0.942 and 0.804, respectively. This confirms that Sensor C made with fibers produced during 60s is more efficient to distinguish among the p53 samples, which reflects the larger number of blue boxes among the four biosensors. From the parallel coordinates, the frequencies 100, 215 and 1000 Hz were selected to construct calibration curves and study the adsorption processes.

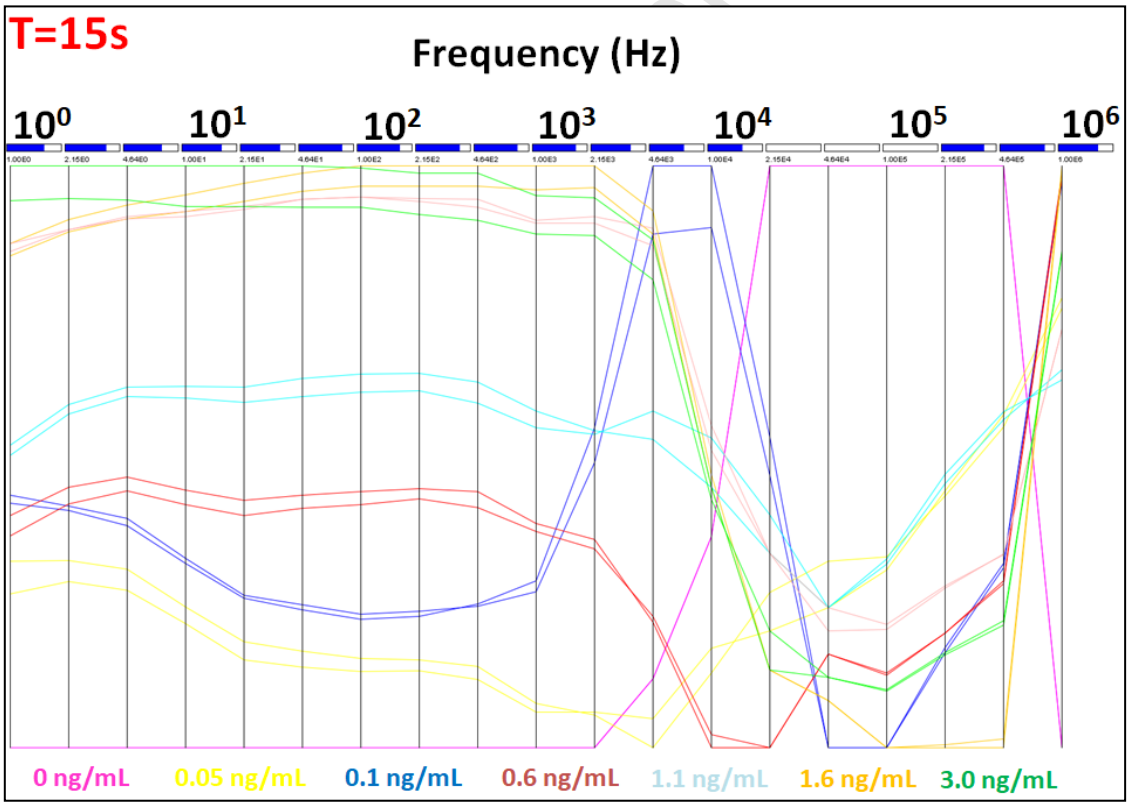

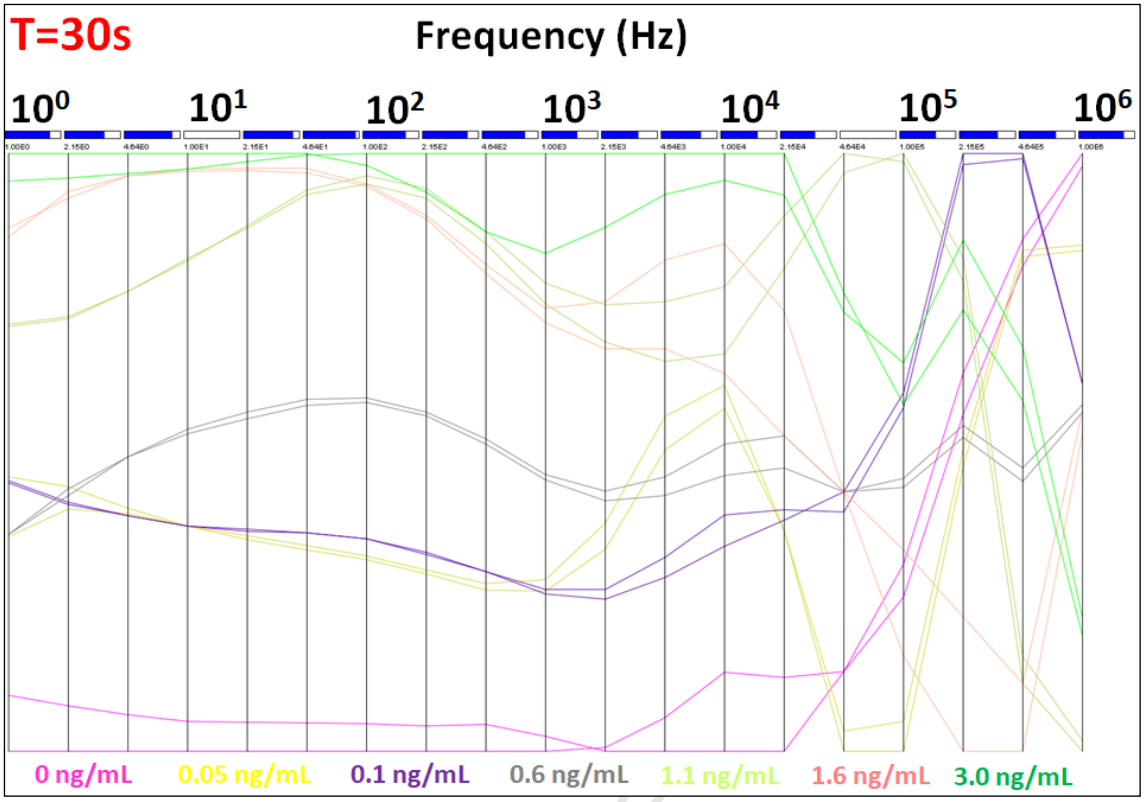
T=30s
Frequency (Hz)
10^0
10^1
10^2
10^3
10^4
10^5
10^6
0 ng/mL
0.05 ng/mL
0.1 ng/mL
0.6 ng/mL
1.1 ng/mL
1.6 ng/mL
3.0 ng/mL

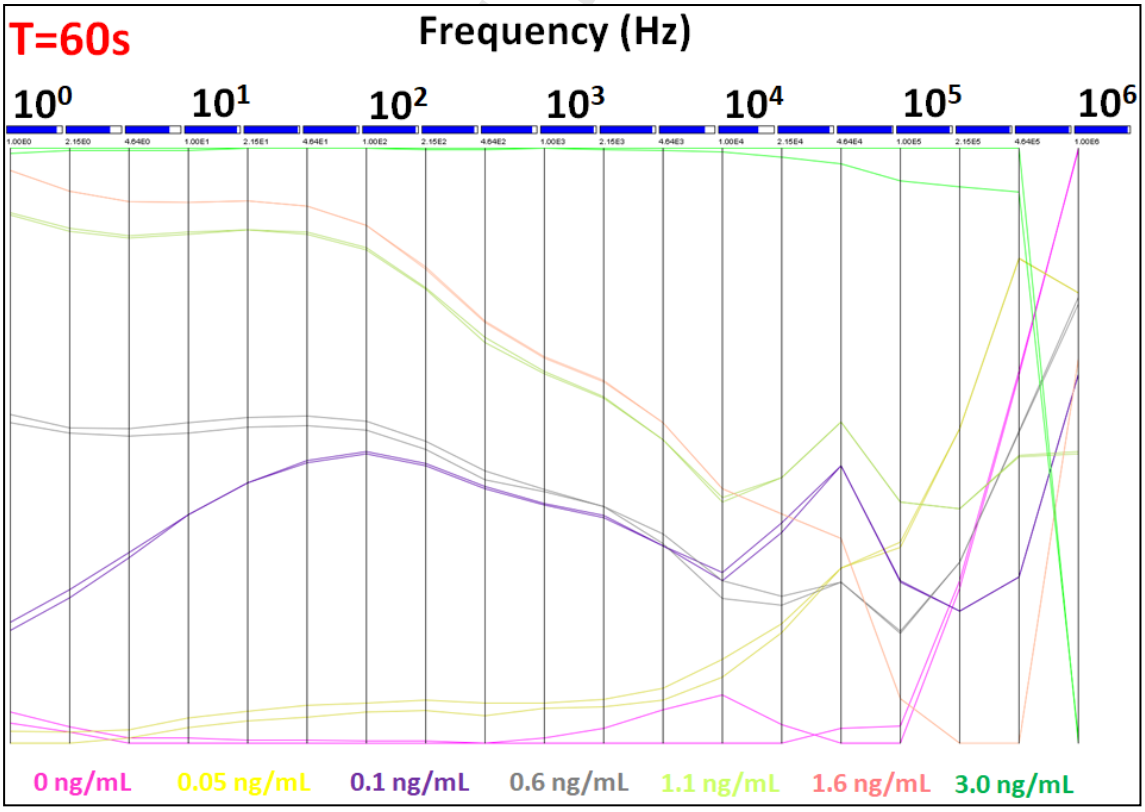
T=60s
Frequency (Hz)
10^0
10^1
10^2
10^3
10^4
10^5
10^6
0 ng/mL
0.05 ng/mL
0.1 ng/mL
0.6 ng/mL
1.1 ng/mL
1.6 ng/mL
3.0 ng/mL

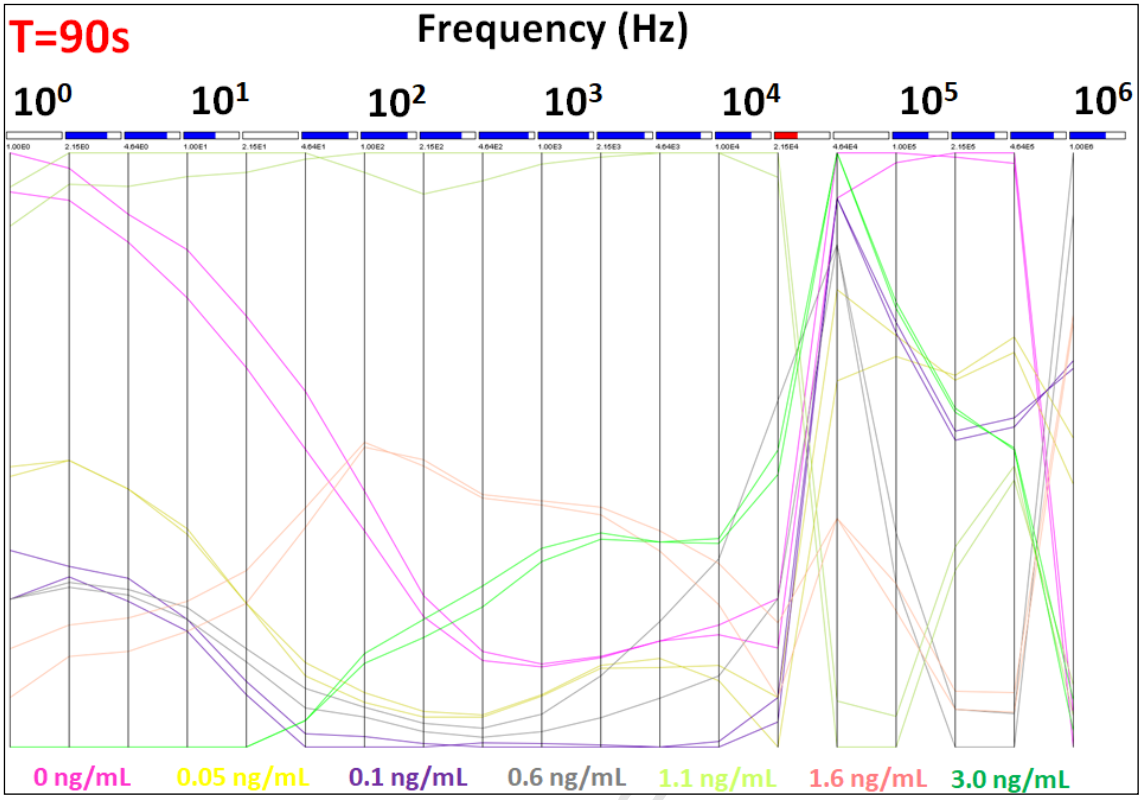

Figure 5: Parallel coordinate (PC) plots for the biosensors A (T=15s), B (T=30s), C (T=60s) and D (T=90s) with silhouette coefficients 0.725, 0.779, 0.942 and 0.804, respectively. The X axis corresponds to frequency while Y corresponds to capacitance values

3.3. Electric Impedance Measurements in Cell Samples with p53 Biomarker

The biosensor efficiency and selectivity for p53 antigen was tested with two types of cell lines, MCF7 and Saos-2, which are p53 positive and negative expressing controls, respectively. IDMAP plots from the capacitance spectra of 6 MCF7 cell concentrations (0; 0.01; 0.1; 1; 10; 100; 500 and 1000 Ucell/mL) were used to evaluate which biosensor was more efficient in detecting p53. In the dimensional projections of Figure 6 and Figure S2 (Supporting Information) there are two behaviors: for biosensor A, there is no distinction between positive and negative samples, i.e. distinct clusters are not formed. This means that Biosensor A cannot be used for p53 detection in cell samples. In biosensors B and C, well-defined clusters are present in multidimensional projections, in which the concentration of cells with p53 increases from left to right of the projection, while the concentration of

negative cells is not organized with increasing cell concentrations. There is good distinction between positive and negative samples for both sensors, but for Biosensor B the samples from cells with 100 Ucell/mL show electrical signals similar to p53 null cells. Thus, biosensor C had the highest p53 detection efficiency in cell samples, making it ideal for future clinical trial applications.

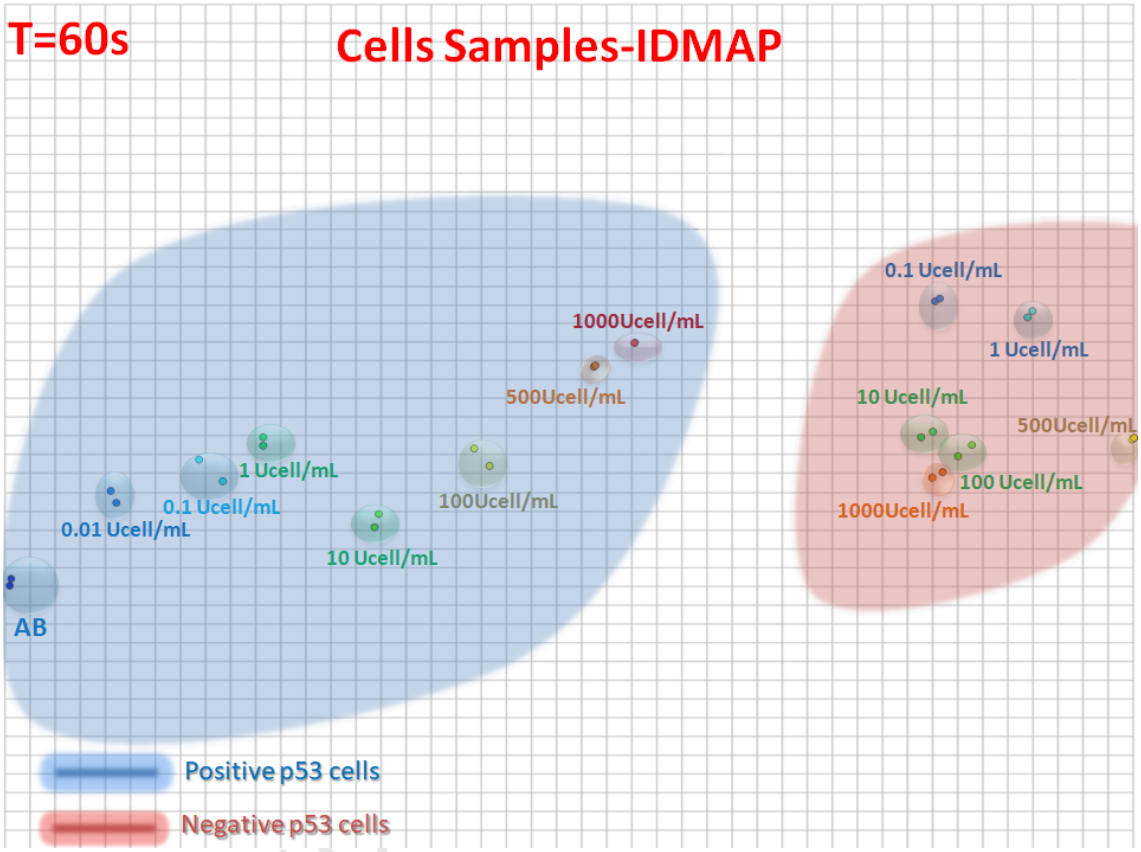

Figure 6: IDMAP plot for the capacitance spectra obtained with biosensor C (Time=60s) for cell culture lysates with (MCF7) or without p53 protein expression (Saos-2). Two clusters were formed on the projection, with negative samples located on the red region and the positive samples on the blue region

3.4. Adsorption Processes Responsible for Biosensing

Adsorption processes in biosensing can be studied theoretically from calibration curves modeled using Freundlich and Langmuir-Freudlich[8,9,34,35] isotherms. One may be surprised by the success of such simple models to fit data from complicated systems with

large interacting molecules. It seems that the specific interaction between antigens and antibodies is sufficiently strong to dominate the overall behavior entirely, in a way that the concentration dependence for the adsorbate is the same as in the adsorption of gas molecules for which these isotherms were proposed. A key feature is the saturation of the available sites, which appears to always occurs in these types of biosensors. The data are normally not fitted with a pure Langmuir isotherm; indeed, one should not expect adsorption to occur as in a monolayer. Since the number of papers describing these adsorption processes for biosensors in the literature is rather limited[7,9,13,36], it has not been possible to establish a general rule to predict which model will be the most appropriate for a given biosensor. Figure 7 illustrates the fitting of calibration curves for biosensors A, B and C at the frequencies with the lowest LODs, with the parameters used for fitting the data being given in the inserts. Biosensor D was not used here because its performance was worse than the others, as already discussed. The concentration dependence was fitted with a Freundlich isotherm for the biosensor containing the PLA fiber matrix deposited during 15 s (Biosensor A), probably owing to the poor homogeneity of the film morphology. For the more homogeneous matrices in Biosensors B and C the data could be fitted with Langmuir-Freundlich isotherms.

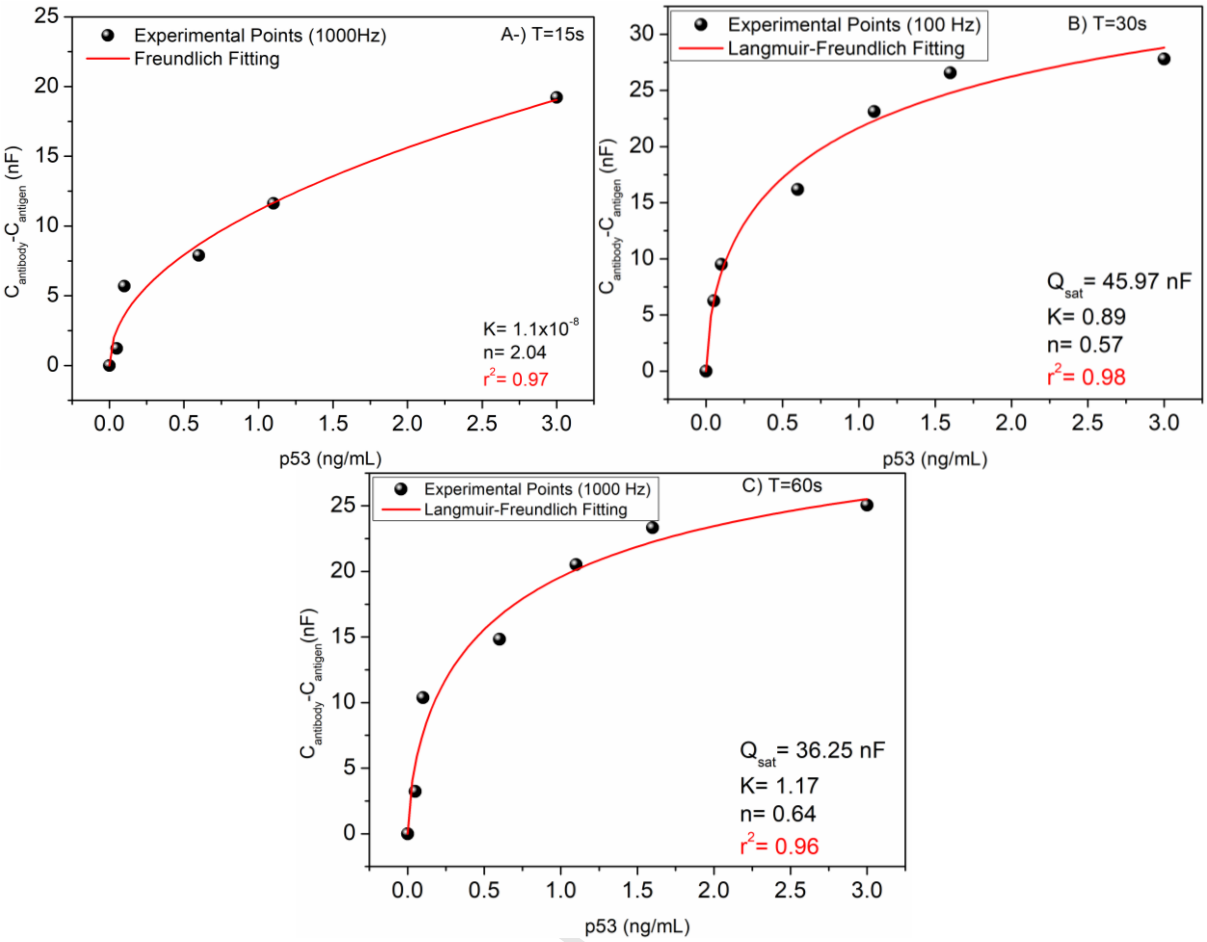

Figure 7: Calibration curves modeled with Freundlich isotherm for (A) biosensor A and Langmuir-Freundlich isotherm for biosensor (B) B and (C) C. From the theoretical values, the capacitance saturation close to 36 nF and the heterogeneity index indicates that this biosensor has a multilayer-forming surface. Biosensor C is more homogeneous than biosensors A and B.

The biosensors reported in this work detect changes in the electrical and optical signals arising from interactions between the active layer immobilized on PLA fibers and the p53 biomarker. The nature of such interactions, which are ultimately responsible for the biosensor performance, can be determined using PM-IRRAS. Figure 8 show PM-IRRAS spectra for films made with PLA fibers during deposition times of 15, 30 and 60s. Three well-defined bands at 1550 cm^{-1}, 1650 cm^{-1} and 1760 cm^{-1} are assigned to amide II (N-H and C-N groups) in p53, amide I group (C=O from p53) and C=O from PLA fibers, respectively[4,8,30,37,38]. The intensity of the carbonyl band from PLA carboxylic acid changes

with p53 concentration, probably due to changes in orientation. The amide bands I and II, related to p53, have their area/intensity decreased from the adsorption on PLA carboxylic acid, thus demonstrating that the AB-AG interaction mechanism is governed by specific interactions.

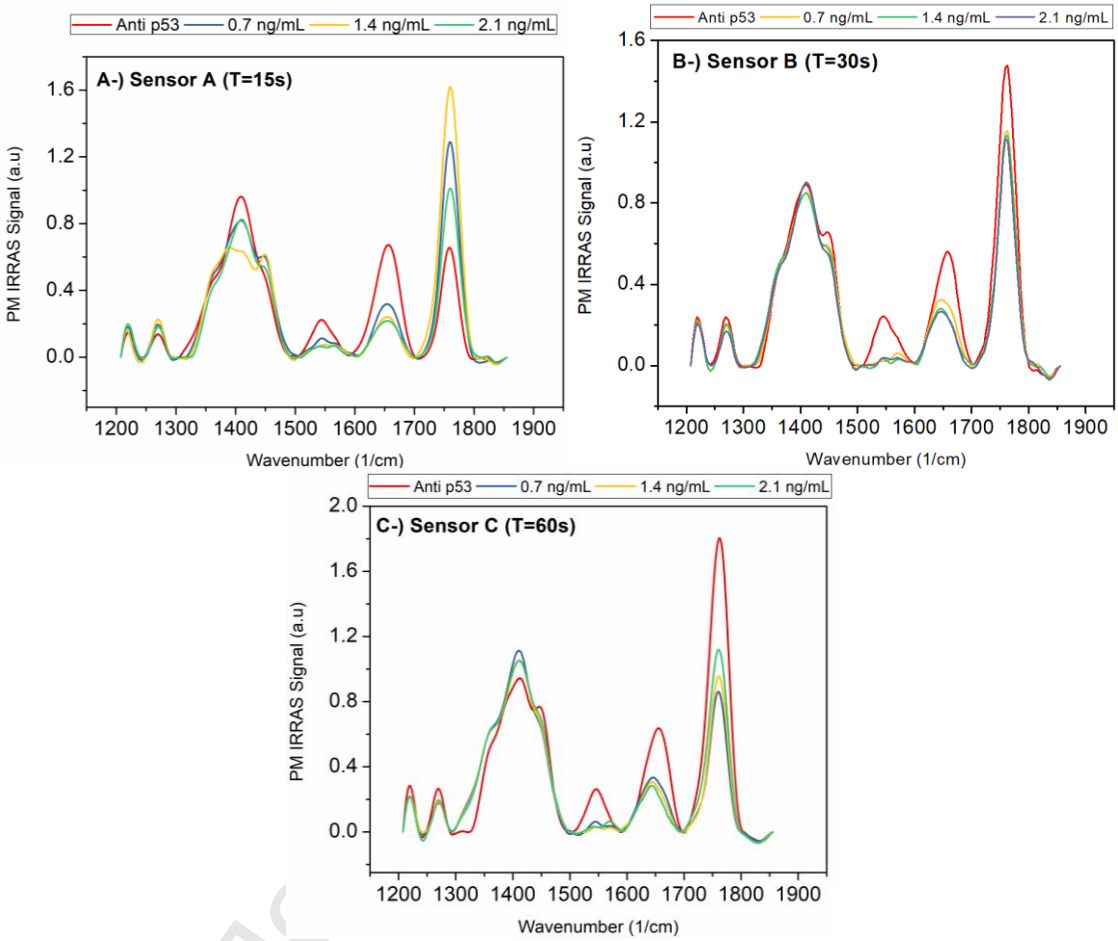

Figure 8: Normalized PM-IRRAS spectra of biosensors constructed from PLA fibers deposited during (A) 15, (B) 30 and (C) 60s. Changes in the molecular orientation of C=O dipole are observed by the decrease in band intensity at 1650 cm^{-1} due to biorecognition between the active layer and the p53 biomarker. The baseline was taken as the clean gold (Au) electrode spectrum.

4. Conclusion

Biosensors constructed from PLA fiber matrices exhibited high sensitivity and selectivity, which depended on the fiber deposition time. The optimized time according to

electrical impedance measurements is 60 s, with superior biosensing performance compared to films built with 15, 30 and 90s. The limit of detection (LoD) could be as low as 11 pg/mL, which is sufficient to detect the p53 biomarker in patient samples, whether in cells or body fluids. Multidimensional projections of the impedance data confirmed the selectivity, especially for biosensor C which was optimized. Using solution blown spun fibers as a matrix for detecting biomarkers represents a low cost, scalable approach that may allow for future dissemination of diagnostic kits in hospitals and even for point-of-care diagnosis.

Conflict of Interests

The authors declare no competing financial interest.

Appendix A. Supplementary Data

Supplementary data to this article can be found online at…

Acknowledgments

The authors are grateful to Brazilian National Council for Scientific and Technological Development (CNPq) (Grant #150985/2017-7, #113757/2018-2, #402287/2013-4 and 303796/2014-6), São Paulo Research Foundation (FAPESP) (Grant #2013/14262-7, #2017/18725-2 and #2018/18953-8), CAPES (001), INEO, and Barretos Cancer Hospital. The authors are also thanks to Maria Helena Piazzetta and Angelo Gobbi (LMF/LNNANO/CNPEM, Brazil) for their assistance in electrode fabrication.

References

(1) Ariga, K.; Nishikawa, M.; Mori, T.; Takeya, J.; Shrestha, L. K.; Hill, J. P. Self-Assembly as a Key Player for Materials Nanoarchitectonics. *Science and Technology of Advanced Materials* 2019, *20* (1), 51–95. https://doi.org/10.1080/14686996.2018.1553108.

(2) Ariga, K.; Matsumoto, M.; Mori, T.; Shrestha, L. K. Materials Nanoarchitectonics at Two-Dimensional Liquid Interfaces. *Beilstein J. Nanotechnol.* 2019, *10*, 1559–1587. https://doi.org/10.3762/bjnano.10.153.

(3) Ariga, K.; Aono, M. *Advanced Supramolecular Nanoarchitectonics*; Elsevier: Netherlands, 2019.

(4) Soares, A. C.; Soares, J. C.; Shimizu, F. M.; Melendez, M. E.; Carvalho, A. L.; Oliveira, O. N. Controlled Film Architectures to Detect a Biomarker for Pancreatic Cancer Using Impedance Spectroscopy. *ACS Appl. Mater. Interfaces* 2015, *7* (46), 25930–25937. https://doi.org/10.1021/acsami.5b08666.

(5) Soares, J. C.; Shimizu, F. M.; Soares, A. C.; Caseli, L.; Ferreira, J.; Oliveira, O. N. Supramolecular Control in Nanostructured Film Architectures for Detecting Breast Cancer. *ACS Appl. Mater. Interfaces* 2015, *7* (22), 11833–11841. https://doi.org/10.1021/acsami.5b03761.

(6) Araujo, F. T.; Peres, L. O.; Caseli, L. Conjugated Polymers Blended with Lipids and Galactosidase as Langmuir–Blodgett Films To Control the Biosensing Properties of Nanostructured Surfaces. *Langmuir* 2019, *35* (22), 7294–7303. https://doi.org/10.1021/acs.langmuir.9b00536.

(7) Soares, A. C.; Soares, J. C.; Rodrigues, V. C.; Follmann, H. D. M.; Arantes, L. M. R. B.; Carvalho, A. C.; Melendez, M. E.; Fregnani, J. H. T. G.; Reis, R. M.; Carvalho, A. L.; et al. Microfluidic-Based Genosensor To Detect Human Papillomavirus (HPV16) for Head and Neck Cancer. *ACS Applied Materials & Interfaces* 2018, *10* (43), 36757–36763. https://doi.org/10.1021/acsami.8b14632.

(8) Soares, A. C.; Soares, J. C.; Shimizu, F. M.; Rodrigues, V. da C.; Awan, I. T.; Melendez, M. E.; Piazzetta, M. H. O.; Gobbi, A. L.; Reis, R. M.; Fregnani, J. H. T. G.; et al. A Simple Architecture with Self-Assembled Monolayers to Build Immunosensors for Detecting the Pancreatic Cancer Biomarker CA19-9. *Analyst* 2018, *143* (14), 3302–3308. https://doi.org/10.1039/C8AN00430G.

(9) Soares, J. C.; Soares, A. C.; Pereira, P. A. R.; Rodrigues, V. da C.; Shimizu, F. M.; Melendez, M. E.; Scapulatempo Neto, C.; Carvalho, A. L.; Leite, F. L.; Machado, S. A. S.; et al. Adsorption According to the Langmuir–Freundlich Model Is the Detection Mechanism of the Antigen P53 for Early Diagnosis of Cancer. *Phys. Chem. Chem. Phys.* 2016, *18* (12), 8412–8418. https://doi.org/10.1039/C5CP07121F.

(10) Oliveira, O. N.; Iost, R. M.; Siqueira, J. R.; Crespilho, F. N.; Caseli, L. Nanomaterials for Diagnosis: Challenges and Applications in Smart Devices Based on Molecular Recognition. *ACS Appl. Mater. Interfaces* 2014, *6* (17), 14745–14766. https://doi.org/10.1021/am5015056.

(11) Ibáñez-Redín, G.; Furuta, R. H. M.; Wilson, D.; Shimizu, F. M.; Materon, E. M.; Arantes, L. M. R. B.; Melendez, M. E.; Carvalho, A. L.; Reis, R. M.; Chaur, M. N.; et al. Screen-Printed Interdigitated Electrodes Modified with Nanostructured Carbon Nano-Onion Films for Detecting the Cancer Biomarker CA19-9. *Materials Science and Engineering: C* 2019, *99*, 1502–1508. https://doi.org/10.1016/j.msec.2019.02.065.

(12) Rodrigues, V. da C.; Comin, C. H.; Soares, J. C.; Soares, A. C.; Melendez, M. E.; Fregnani, J. H. T. G.; Carvalho, A. L.; Costa, L. da F.; Oliveira, O. N. Analysis of Scanning Electron Microscopy Images To Investigate Adsorption Processes Responsible for Detection of Cancer Biomarkers. *ACS Appl. Mater. Interfaces* 2017, *9* (7), 5885–5890. https://doi.org/10.1021/acsami.6b16105.

(13) Thapa, A.; Soares, A. C.; Soares, J. C.; Awan, I. T.; Volpati, D.; Melendez, M. E.; Fregnani, J. H. T. G.; Carvalho, A. L.; Oliveira, O. N. Carbon Nanotube Matrix for Highly Sensitive Biosensors To Detect Pancreatic Cancer Biomarker CA19-9. *ACS*

Appl. Mater. Interfaces 2017, *9* (31), 25878–25886. https://doi.org/10.1021/acsami.7b07384.

(14) Jeong, S.; Barman, S. C.; Yoon, H.; Park, J. Y. A Prostate Cancer Detection Immunosensor Based on Nafion/Reduced Graphene Oxide/Aldehyde Functionalized Methyl Pyridine Composite Electrode. *J. Electrochem. Soc.* 2019, *166* (12), B920–B926. https://doi.org/10.1149/2.0361912jes.

(15) Han, L.; Wang, D.; Yan, L.; Petrenko, V. A.; Liu, A. Specific Phages-Based Electrochemical Impedimetric Immunosensors for Label-Free and Ultrasensitive Detection of Dual Prostate-Specific Antigens. *Sensors and Actuators B: Chemical* 2019, *297*, 126727. https://doi.org/10.1016/j.snb.2019.126727.

(16) Ding, S.-N.; Wang, X.-Y.; Lu, W.-X. Switches-Controlled Bipolar Electrode Electrochemiluminescence Arrays for High-Throughput Detection of Cancer Biomarkers. *Journal of Electroanalytical Chemistry* 2019, *844*, 99–104. https://doi.org/10.1016/j.jelechem.2019.05.021.

(17) Thangamuthu, M.; Hsieh, K. Y.; Kumar, P. V.; Chen, G.-Y. Graphene- and Graphene Oxide-Based Nanocomposite Platforms for Electrochemical Biosensing Applications. *IJMS* 2019, *20* (12), 2975. https://doi.org/10.3390/ijms20122975.

(18) Proença, C. A.; Baldo, T. A.; Freitas, T. A.; Materón, E. M.; Wong, A.; Durán, A. A.; Melendez, M. E.; Zambrano, G.; Faria, R. C. Novel Enzyme-Free Immunomagnetic Microfluidic Device Based on Co0.25Zn0.75Fe2O4 for Cancer Biomarker Detection. *Analytica Chimica Acta* 2019, *1071*, 59–69. https://doi.org/10.1016/j.aca.2019.04.047.

(19) Wilson, D.; Materón, E. M.; Ibáñez-Redín, G.; Faria, R. C.; Correa, D. S.; Oliveira, O. N. Electrical Detection of Pathogenic Bacteria in Food Samples Using Information Visualization Methods with a Sensor Based on Magnetic Nanoparticles Functionalized with Antimicrobial Peptides. *Talanta* 2019, *194*, 611–618. https://doi.org/10.1016/j.talanta.2018.10.089.

(20) Soares, J. C.; Iwaki, L. E. O.; Soares, A. C.; Rodrigues, V. C.; Melendez, M. E.; Fregnani, J. H. T. G.; Reis, R. M.; Carvalho, A. L.; Corrêa, D. S.; Oliveira, O. N. Immunosensor for Pancreatic Cancer Based on Electrospun Nanofibers Coated with Carbon Nanotubes or Gold Nanoparticles. *ACS Omega* 2017, *2* (10), 6975–6983. https://doi.org/10.1021/acsomega.7b01029.

(21) Rahman, Md. M.; Ahammad, A. J. S.; Jin, J.-H.; Ahn, S. J.; Lee, J.-J. A Comprehensive Review of Glucose Biosensors Based on Nanostructured Metal-Oxides. *Sensors* 2010, *10* (5), 4855–4886. https://doi.org/10.3390/s100504855.

(22) Paschoalin, R. T.; Traldi, B.; Aydin, G.; Oliveira, J. E.; Rütten, S.; Mattoso, L. H. C.; Zenke, M.; Sechi, A. Solution Blow Spinning Fibres: New Immunologically Inert Substrates for the Analysis of Cell Adhesion and Motility. *Acta Biomaterialia* 2017, *51*, 161–174. https://doi.org/10.1016/j.actbio.2017.01.020.

(23) da Silva Parize, D. D.; Foschini, M. M.; de Oliveira, J. E.; Klamczynski, A. P.; Glenn, G. M.; Marconcini, J. M.; Mattoso, L. H. C. Solution Blow Spinning: Parameters Optimization and Effects on the Properties of Nanofibers from Poly(Lactic Acid)/Dimethyl Carbonate Solutions. *J Mater Sci* 2016, *51* (9), 4627–4638. https://doi.org/10.1007/s10853-016-9778-x.

(24) Medeiros, E. S.; Glenn, G. M.; Klamczynski, A. P.; Orts, W. J.; Mattoso, L. H. C. Solution Blow Spinning: A New Method to Produce Micro- and Nanofibers from Polymer Solutions. *J. Appl. Polym. Sci.* 2009, *113* (4), 2322–2330. https://doi.org/10.1002/app.30275.

(25) Kastenhuber, E. R.; Lowe, S. W. Putting P53 in Context. *Cell* 2017, *170* (6), 1062–1078. https://doi.org/10.1016/j.cell.2017.08.028.

(26) Donehower, L. A.; Soussi, T.; Korkut, A.; Liu, Y.; Schultz, A.; Cardenas, M.; Li, X.; Babur, O.; Hsu, T.-K.; Lichtarge, O.; et al. Integrated Analysis of TP53 Gene and Pathway Alterations in The Cancer Genome Atlas. *Cell Reports* 2019, *28* (5), 1370-1384.e5. https://doi.org/10.1016/j.celrep.2019.07.001.

(27) Paulovich, F. V.; Moraes, M. L.; Maki, R. M.; Ferreira, M.; Oliveira Jr., O. N.; de Oliveira, M. C. F. Information Visualization Techniques for Sensing and Biosensing. *Analyst* 2011, *136* (7), 1344. https://doi.org/10.1039/c0an00822b.

(28) Riul Jr., A.; Dantas, C. A. R.; Miyazaki, C. M.; Oliveira Jr., O. N. Recent Advances in Electronic Tongues. *Analyst* 2010, *135* (10), 2481. https://doi.org/10.1039/c0an00292e.

(29) Inselberg, A.; Dimsdale, B. Parallel Coordinates: A Tool for Visualizing Multi-Dimensional Geometry. In *Proceedings of the First IEEE Conference on Visualization: Visualization `90*; IEEE Comput. Soc. Press: San Francisco, CA, USA, 1990; pp 361–378. https://doi.org/10.1109/VISUAL.1990.146402.

(30) Oliveira, J. E.; Mattoso, L. H. C.; Orts, W. J.; Medeiros, E. S. Structural and Morphological Characterization of Micro and Nanofibers Produced by Electrospinning and Solution Blow Spinning: A Comparative Study. *Advances in Materials Science and Engineering* 2013, *2013*, 1–14. https://doi.org/10.1155/2013/409572.

(31) Lvovich, V. F. *Impedance Spectroscopy: Applications to Electrochemical and Dielectric Phenomena*; Wiley: Hoboken, N.J, 2012.

(32) Barsoukov, E., Macdonald, J. R. *Impedance Spectroscopy: Theory, Experiment, and Applications*, Wiley-Interscience: Hoboken, N.J, 2005.

(33) Sousa, M. A.; Siqueira-Junior, J. R.; Vercik, A.; Schöning, M. J.; Oliveira Jr, O. N. Determining the optimized layer-by-layer film architecture with dendrimer/carbon nanotubes for field-effect sensors. *IEEE Sensors Journal* 2017, 17 (6), 1735-1740. https://doi.org/10.1109/JSEN.2017.2653238.

(34) Jeppu, G. P.; Clement, T. P. A Modified Langmuir-Freundlich Isotherm Model for Simulating PH-Dependent Adsorption Effects. *Journal of Contaminant Hydrology* 2012, *129–130*, 46–53. https://doi.org/10.1016/j.jconhyd.2011.12.001.

(35) Turiel, E.; Perez-Conde, C.; Martin-Esteban, A. Assessment of the Cross-Reactivity and Binding Sites Characterisation of a Propazine-Imprinted Polymer Using the Langmuir-Freundlich Isotherm. *Analyst* 2003, *128* (2), 137–141. https://doi.org/10.1039/b210712k.

(36) Lee, H. J.; Wark, A. W.; Corn, R. M. Creating Advanced Multifunctional Biosensors with Surface Enzymatic Transformations. *Langmuir* 2006, *22* (12), 5241–5250. https://doi.org/10.1021/la060223o.

(37) Colthup, N. B.; Daly, L. H.; Wiberley, S. E. *Introduction to Infrared and Raman Spectroscopy*, 3rd ed.; Academic Press: Boston, 1990.

(38) Więckowski, A., Korzeniewski, C., Braunschweig, B. *Vibrational Spectroscopy at Electrified Interfaces*, Wiley: Hoboken, New Jersey, 2013.

Author Contributions

Andrey: Conceptualization; Data curation; Formal analysis; Investigation; Methodology; Project administration; Writing – review & editing. (responsible to performed experiments, data analysis, prepared the figures and wrote the manuscript).

Juliana: Formal analysis; Investigation; Methodology; Writing – review & editing. (responsible to carried out the statistical analysis with information visualization techniques and analyzed the corresponding data).
Rafaella: Formal analysis; Investigation; Methodology; Writing – review & editing (performed the Solution Blow Spun Fibers of Poly(Lactic Acid) Fibers and fibers characterizations)**.**
Valquiria: Formal analysis; Investigation; Methodology; Writing – review & editing (performed the PM-IRRAS measurements and Adsorption Mechanism analysis).
Matias: Investigation; Methodology; Writing – review & editing (performed the extraction, cultivation preparation and characterization of the MCF7 Saos-2 human cell samples at Barretos Cancer Hospital).
Rui: Investigation; Methodology; Project administration; Writing – review & editing (responsible for the experiments and data analysis at Barretos Cancer Hospital).
Andre: Investigation; Methodology; Project administration; Writing – review & editing (responsible for the experiments and data analysis at Barretos Cancer Hospital).
Luiz Henrique: Formal analysis; Investigation; Methodology; Supervision; Project administration; Writing – review & editing (responsible for the experiments and data analysis at Embrapa Instrumentation).
Osvaldo: Formal analysis; Investigation; Methodology; Supervision; Funding acquisition; Project administration; Writing – review & editing (was the research coordinator and edited the manuscript).
All authors proofread the manuscript.

Declaration of competing interest

The authors declare that they have no known competing financial interests or personal relationships that could have appeared to influence the work reported in this paper.

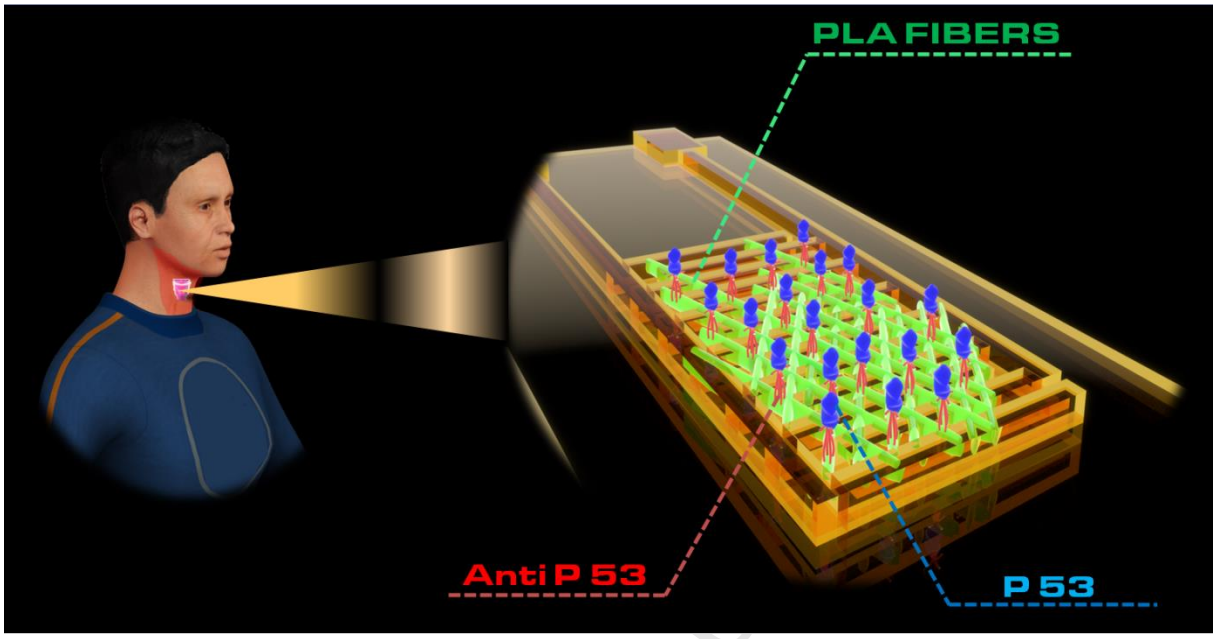

Graphical abstract

Highlights

* Low-cost biosensors fabricated with PLA fibers used for detecting p53 biomarker.
* Fibers produced by SB-Spinning explored for the first time as biosensor matrices.
* Optimized performance for fibers deposited during 60 s on interdigitated electrodes.
* Biosensors sensitive to p53, with Limit of Detection of 11pM.